Combustion Science and Technology

ISSN: 0010-2202 (Print) 1563-521X (Online) Journal homepage: www.tandfonline.com/journals/gcst20

Numerical Studies on Minimum Ignition Energies of Lean Primary Reference Fuels at Elevated Pressure

Chunwei Wu, Robert Schießl & Ulrich Maas

To cite this article: Chunwei Wu, Robert Schießl & Ulrich Maas (10 Apr 2026): Numerical Studies on Minimum Ignition Energies of Lean Primary Reference Fuels at Elevated Pressure, Combustion Science and Technology, DOI: 10.1080/00102202.2026.2654694

To link to this article: https://doi.org/10.1080/00102202.2026.2654694

Published online: 10 Apr 2026.

COMBUSTION SCIENCE AND TECHNOLOGY
https://doi.org/10.1080/00102202.2026.2654694

Numerical Studies on Minimum Ignition Energies of Lean Primary Reference Fuels at Elevated Pressure

Chunwei Wu, Robert Schießl, and Ulrich Maas

Institute of Technical Thermodynamic, Karlsruhe Institute of Technology, Karlsruhe, Germany

ABSTRACT

The minimum ignition energy (MIE) is a crucial parameter that signifies the minimum external energy required for a successful-induced ignition. Focusing on primary reference fuel (PRF), a popular gasoline surrogate, we employed numerical simulations to investigate the flame initiation and early flame propagation process at elevated pressures. This study aims to explore the flame initiation and evolution after external energy and the dependence of MIE on pressure and mixture composition. It uses numerical simulations involving detailed treatment of chemistry and molecular transport for the solution of the conservation equations during ignition and the early stages of flame propagation. Due to the low temperature chemistry (LTC) at elevated pressure, four distinct flame types can be observed after ignition energy deposition: ignition failure, cool flame ignition and extinction, two-stage ignition, and hot flame ignition. In contrast to 1 bar conditions, where the hot flame might quench due to curvature, the hot flame is always self-sustained at elevated pressure for the conditions investigated in this work. The MIE for a self-sustained flame, MIE_{prop} at low pressure increases with pressure, but experiences a sudden drop at some specific pressure, when the cool flame can evolve into a hot flame. The fact that the LTC of n-heptane is much more stronger than iso-octane affects the MIE_{prop} of PRF mixtures. Our results corporate the significance of LTC for induced ignition and early flame propagation processes of PRFs at elevated pressure, bearing implications in practical combustion engines and safety considerations.

ARTICLE HISTORY
Received 7 November 2025
Revised 16 January 2026
Accepted 30 January 2026

KEYWORDS
Induced ignition; minimum ignition energy; primary reference fuels; laminar premixed flame

Introduction

Ignition and early flame propagation studies are not only important for to developing efficient and clean combustion strategies, but are also crucial for safety considerations. Understanding the ignition process and its underlying physical and chemical mechanisms is relevant for various practical applications, including internal combustion engines.

Minimum ignition energy (MIE), which is the minimum required energy for a successful flame initiation, is characteristic for induced ignition (Warnatz et al. 2006a). The minimum ignition energy and its dependence on temperature, pressure and mixture composition were studied numerically and experimentally in the past (Moorhouse et al. 1974; Maas U and

CONTACT Chunwei Wu chunwei.wu@kit.edu Institute of Technical Thermodynamic, Karlsruhe Institute of Technology, Engelbert-Arnold-Straße 4, Karlsruhe 76131, Germany

Warnatz J 1988; Lewis and Von Elbe 2012; Wu et al. 2021, 2023), for a summary see e.g. (Uchman and Werle 2018).

Primary reference fuels (PRF, mixtures of iso-octane and n-heptane) are popular surrogates for gasoline. They are characterized by the research octane number (RON), which is the volume-percentage of iso-octane in the mixture. RON = 0 corresponds to n-heptane and RON = 100 corresponds to iso-octane Edgar (1927). Considering efficiency improvement and emission reduction, lean premixed ignition of PRF is of great interest. Detailed and reduced chemical kinetic mechanisms of PRF were developed and validated with parameters like ignition delay times and laminar flame speeds (Curran et al. 1998a, 1998b; Curran et al. 2002; Andrae 2008; Andrae and Head 2009). The autoignition process and steady flame propagation of PRFs are well studied both numerically and experimentally (Davis and Law 1998; Kumar et al. 2007; Kelley et al. 2011; Yin et al. 2022).

In our previous study, we focused on the spark ignition process of premixed fuel-air mixtures, and the transition from a flame kernel to a self-sustained flame at 1 bar (Wu et al. 2023). The dependence of MIE on RON at 1 bar was investigated both in experiments and simulations. For spherical geometry, flame extinction might exist because of the strong diffusion caused by large curvature right after ignition (Wu et al. 2021). It was observed both in experiments and simulations, that at 1 bar, MIE depends only weakly on RON until a certain RON_{lim}, starting from RON_{lim}, MIE increases rapidly with RON. This can be explained by the different oxidation mechanisms of iso-octane and n-heptane (Wu et al. 2023). While 1 bar conditions are not representative of most practical combustion systems using PRF-type fuels, they serve as an important baseline for fundamental ignition studies.

In this study, elevated-pressure simulations are presented, which are more relevant to practical applications. At elevated pressures, for hydrocarbon fuels like PRF, low temperature chemistry (LTC) is very important, and negative temperature coefficient (NTC) behavior is observed (Griffiths and Scott 1987; Müller et al. 1992; Curran et al. 1998b; Dagaut and Togbé 2009), which is closely related to engine knock (Griffiths et al. 2002). With simulations and HCCI experiments, the influence of LTC on auto-ignition processes of large hydrocarbon fuels like PRF was well studied (Ju et al. 2011; Sun et al. 2015; Pan et al. 2016). Cool flame and two-stage ignition for large hydrocarbon fuels like PRF were observed (Peters et al. 2002; Stagni et al. 2018; Zhong et al. 2020; Ju 2021). It was found that the existence of cool flames extended the flammability limit (Ju 2017; Liang and Law 2017).

Recent experimental studies using high-speed optical diagnostics combined with simulations have further advanced the understanding of cool-flame propagation and LTC-dominated ignition under high-pressure conditions. In particular, Sim et al. investigated cool-flame dynamics, early-stage reaction pathways, and cool-to-hot flame transition for hydrocarbon and PRF fuels, demonstrating the critical role of LTC intermediates and pressure effects on ignition behavior (Sim et al. 2021, 2023, 2024, 2025). These studies provide state-of-the-art experimental baselines for high-pressure cool-flame ignition.

However, there are fewer studies investigating the effect of LTC for the transition from induced ignition to a self-sustained flame of PRFs at elevated pressure. The following questions remain open:

- What is the behavior of the system after the deposition of energy at elevated pressure? Does LTC play an important role in determination of different flame regimes? Are there any differences in comparison to the flame regimes at 1 bar?

- How does pressure affect the MIE for a self-sustained flame of PRFs?
- How does the MIE of PRFs depend on RON at elevated pressures? Does the same phenomenon at 1 bar also exist?

To answer these questions, numerical simulations of flame initiation and early flame propagation of premixed PRF/air mixtures at pressure ranging from 3 bar to 25 bar and an initial temperature of 373 K with spherical geometry are conducted, considering detailed chemical kinetics and detailed transport process. Diffusion caused by concentration gradient is modeled using a reduced Stefan formulation with effective mixture-averaged diffusion coefficients derived from binary diffusivities (Warnatz et al. 2006b; Hirschfelder et al. 1964; Bird et al. 2002). Thermo-diffusion (Soret effect) is accounted for by an additional temperature-gradient-driven flux term using the Paul–Warnatz formulation (Paul and Warnatz 1998). The initial temperature of 373 K is identical to the initial temperature used in our former ignition study at 1 bar (Wu et al. 2023), and is important for safety-related issues (Tanoue et al. 2017). This study focuses on fundamental ignition and flame propagation processes under lean conditions relevant to spark-ignition (SI) engines with premixed fuel/air mixtures. The objective is to improve insight into the role of interacting chemical processes and transport phenomena during ignition of PRFs at elevated pressures, especially regarding the influence of low temperature chemistry.

Numerical methodology

In this study, the ignition and flame propagation process is modeled with an updated version the in-house code INSFLA (Maas U and Warnatz J 1988). This code solves the conservation equations for a reacting flow in one-dimensional configurations, using detailed chemical kinetics and detailed transport processes. INSFLA uses an adaptive spatial grid and an adaptive time-stepping with error control. A space- and time-dependent ignition source term can be implemented. The simulations use a spherically symmetric domain, which is consistent with our previous study at 1 bar (Wu et al. 2023). Symmetric boundary conditions at the center and non-catalytic, adiabatic outer boundary conditions for species and temperature are applied. While this one-dimensional laminar formulation neglects multidimensional effects and ignition kernel distortions that may arise in practical systems, it is well suited for isolating the fundamental chemical – diffusive mechanisms governing forced ignition and MIE scaling, the significantly reduced computational cost compared to two- or three-dimensional simulations enables detailed parametric studies to better understand the underlying physics.

The initial condition for species and temperature are homogeneous fuel/air mixtures with an initial temperature $T_0 = 373\,\mathrm{K}$ throughout the entire domain. In this study, a mixture with $\phi = 0.8$ is selected as a representative case, as fuel-lean conditions are typical of practical engine operation. In addition, several test cases with $\phi = 1.2$ demonstrate that the low-temperature chemistry and transport effects discussed here remain qualitatively applicable beyond strictly fuel-lean conditions. The investigated pressure range spans $p = 3 - 25\,\mathrm{bar}$, aimed at enhancing the understanding of ignition process at elevated pressure, including the influence of low temperature chemistry. A constant pressure assumption is applied in all simulations because the ignition times considered in this

study are sufficiently long ($\tau_s = 1 \times 10^{-4}$ s) to allow pressure equilibration within the reacting system, for which the uniform-pressure approximation is valid (Maas U and Warnatz J 1988). The air composition used in this study comprises 21%O_2 and 79%N_2.

The investigated fuel in this study is PRF, characterized by the research octane number, which corresponds to the volumetric percentage of iso-octane. In the result section, most of the detailed analyses focus on PRF0 and PRF100. This choice is motivated by the fact that the ignition characteristics and low-temperature chemistry of intermediate PRF mixtures are primarily governed by the relative contributions of these two limiting components. Accordingly, the dependence of MIE on RON is captured by systematically varying the relative dominance of n-heptane and iso-octane, with intermediate PRF mixtures expected to exhibit MIE trends bounded by the two extremes.

Lean mixtures are studied here because of their attractive emission reduction and high efficiency (see e.g. (Dunn-Rankin 2011)). We use the mechanism based on a semi-detailed chemical kinetics model for tolune reference fuels (TRF) with 137 species and 633 reactions for the simulation of PRF (Andrae JC, Brinck T, et al. 2008), which also contains mechanism of PRF. This mechanism has undergone validation with homogeneous charge compression ignition (HCCI) experiments and is very popular for simulations of gasoline surrogate fuel (see e.g. (Yin et al. 2022)). To assess the sensitivity to the choice of chemical kinetic mechanism, the minimum ignition energy was additionally evaluated at one representative condition using the LLNL PRF mechanism (Curran et al. 1998b). The resulting MIE was found to be very similar to that obtained with the primary mechanism (for n-heptane/air mixture with $\phi = 0.8$, $T_0 = 373$ K, and $p_0 = 5$ bar, the MIE calculated with current mechanism is 30.2 mJ, and the MIE calculated with LLNL mechanism is 30.9 mJ), confirming that the main trends of ignition energy dependence on RON and pressure are robust. We note, however, that low-temperature chemistry pathways could exhibit some mechanism dependence, and the detailed radical evolution may differ for other mechanisms, which could influence secondary LTC-related phenomena.

During the ignition duration ($\tau_s = 1 \times 10^{-4}$ s), an external source term is introduced. This term is characterized by a power density $\dot{q} = \dot{q}(r,t)$ which follows an exponential form derived from experimental source profiles of analogous ignition processes (Maas U and Warnatz J 1988):

$$\begin{aligned} \dot{q} &= \dot{q}_{\max} e^{-\left(\frac{r}{r_s}\right)^8} \quad for \quad 0 < t \leq \tau_s \\ \dot{q} &= 0 \qquad\qquad\qquad for \quad t > \tau_s \end{aligned} \tag{1}$$

r_s represents the ignition radius. In this study, the value $r_s = 1.5$mm was chosen, consistent with our previous study at 1 bar, to allow better comparison between ignition at elevated pressures and at 1 bar. Note that the MIE is sensitive to the ignition radius, as the ignition volume and diffusion are both affected by r_s. While different kernel sizes may alter the absolute MIE values, the present choice enables a consistent investigation of pressure and LTC effects on ignition behavior. The influence of r_s on MIE is further analyzed in the Results section (Figure 4). q_{max} is the maximum ignition power density.

For spherical geometry, the ignition energy E_{ig} has units of J.

$$E_{ig} = \int_0^{r_s} \int_0^{\tau_s} 4\pi r^2 \dot{q} dr dt \tag{2}$$

The maximal ignition energy density q_{max}, which is $\dot{q}_{\max}$ times ignition duration τ_s, is

$$q_{max} = \dot{q}_{\max} \cdot \tau_s = 0.889 \frac{E_{ig}}{\frac{4}{3}\pi r_s^3}. \tag{3}$$

The factor 0.889 results from integrating the exponential function $e^{-(r/r_s)^8}$ over the spherical domain $0 \leq r \leq r_s$. This coefficient thus accounts for the non-uniform spatial distribution of the ignition power density defined in Eq. (1).

To distinguish between flame propagation and thermal expansion in the evaluation of simulation results, a mass-based Lagrangian coordinate Ψ is used (Maas U and Warnatz J 1988; Maas U, Raffel B, et al. 1988) instead of the spatial coordinate r; the advantages of using Ψ instead of r are explained in detail in (Wu et al. 2023). For spherical geometry, there is (Maas U, Raffel B, et al. 1988)

$$\left(\frac{\partial \Psi}{\partial r}\right)_t = \rho r^2 \tag{4}$$

where ρ is the density of the mixture. Ψ_{r_f} represents Ψ at the flame front, which is defined as the distance between the center ($r = 0$) and the peak of the heat release rate.

The outcome of the simulations are spatio-temporal profiles of pressure, temperature and chemical composition during and after ignition.

Results and discussions

Four qualitatively different ignition scenarios

The external energy source raises the temperature in the ignition volume. This may result in the formation of a flame kernel, i.e., in the ignition of the gas mixture in the ignition volume. The resulting flame kernel might quench, or propagate and evolve into a self-sustained flame.

Figure 1 shows four different types of the spatio-temporal evolution of the temperature. The ignition source, which is active from $t = 0$ to $t = 10^{-4}s$, causes a rise in the maximum temperature for all four cases. The temperature profiles during energy deposition are highlighted in blue.

For Type I, the low ignition energy causes only a minor temperature increase, insufficient to trigger fast chemical reactions in the spark volume. As a result, the mixture cools rapidly due to dissipative losses, and ignition fails because the reaction rate remains below the critical level required for ignition kernel formation.

For Type II, the gas temperature increases by approximately 100 K after the external energy deposition. This indicates the onset of a weakly exothermic stage, forming a transient flame kernel where low-temperature chemistry dominates. The chemical reactions proceed slowly due to the limited buildup of reactive radicals, resulting in weak heat release and only partial oxidation of the mixture. Consequently, the temperature does not reach the threshold for high-temperature chain branching, and the transient cool-flame kernel quenches (Ju 2021).

For Type III, a similar first-stage ignition occurs as in Type II, producing a cool flame governed by low-temperature peroxy chemistry. However, the accumulated intermediates and radicals (e.g., HO_2 and OH) gradually increase the reactivity of the mixture. Once the

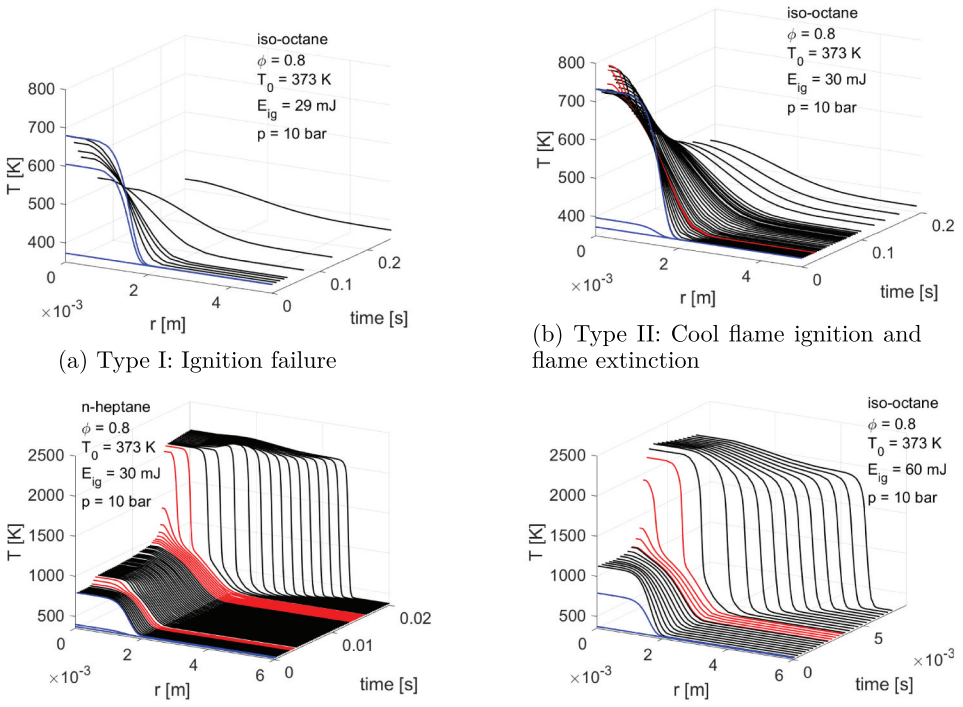

(a) Type I: Ignition failure

(b) Type II: Cool flame ignition and flame extinction

(c) Type III: Two-stage ignition

(d) Type IV: Hot flame ignition

Figure 1. Spatio-temporal evolution of the temperature for four different types. Red profiles indicate ignition stages.

temperature reaches the critical threshold for high-temperature oxidation, a second-stage ignition follows, characterized by rapid chain branching and a steep temperature rise of approximately 1500 K, resulting in complete fuel oxidation to CO_2 and H_2O (Warnatz et al. 2006a; Curran et al. 1998a).

For Type IV, the ignition energy raises the local temperature directly above 1000 K, bypassing the low-temperature reaction regime. This type is termed hot flame initiation.

Previous experimental studies on iso-octane/air mixtures have shown that LTC can occur over a wide range of equivalence ratios, from very lean ($\phi < 0.05$) to moderately rich mixtures, and that strength of low-temperature chemistry (LTC) is generally dependent on the equivalence ratio (Bajwa et al. 2025). Based on these findings, we expect that while the absolute MIE values would vary with ϕ, the qualitative behavior of the four ignition regimes identified here (Type 1–4) would remain similar, though the transition points between regimes may shift as the mixture becomes leaner or richer. This expectation is further supported by additional simulations performed at $\phi = 1.2$, which also exhibit the same four ignition regimes.

The flame structure of the hot and cool flame of n-heptane is shown in Figure 2. The difference is clearly observed: Although the peak of the OH mass fraction of the cool flame is about 1000 times smaller than the hot flame, the peak of the HO_2 and $C_7H_{15}O_2H$ mass fraction of the cool flame is 3 times larger than the hot flame, and the peak of the H_2O_2 mass fraction of the cool flame is 10 times larger than the hot flame. This indicates the

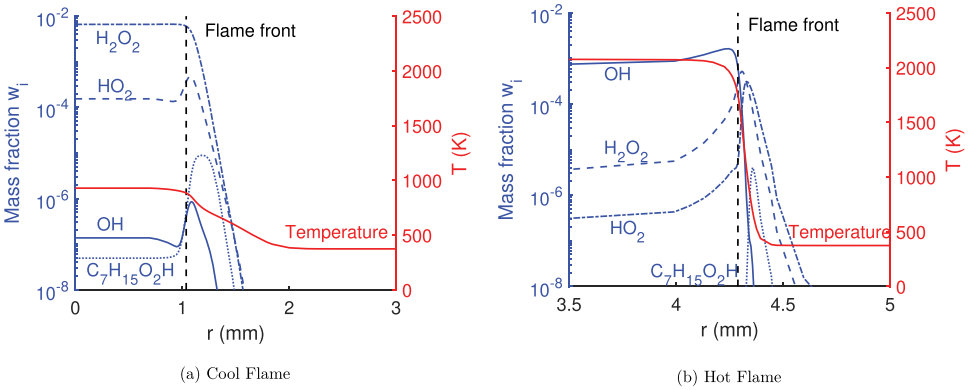

Figure 2. The temperature profile and mass fraction profiles of oh, H_2O_2, HO_2, and $C_7H_{15}O_2H$ for the cool and hot flame of n-heptane at $\phi = 0.8$, $p = 10$ bar, $T_0 = 373$ K, using spherical geometry with $r_s = 1.5$ mm.

importance of the reactions with HO_2, H_2O_2, and $C_7H_{15}O_2H$ radicals and confirms that the cool flame is dominated by the low-temperature chemistry of n-heptane. Similar qualitative trends were observed for iso-octane and PRF mixtures at $T_0 = 373$ K and elevated pressures, and the key features discussed for n-heptane also apply to these fuels (not shown).

Dependence of MIE of n-heptane and iso-octane on pressure

Figure 3 shows the dependence of MIE for both n-heptane/air mixtures and iso-octane/air mixtures on pressure. Ignition types III and IV (which both create a self-sustained flame) are highlighted in red. Ignition types I and II (which do not create self-sustained flames) are highlighted in blue. MIE_{cool} and MIE_{hot} are defined for a successful flame kernel formation of a cool flame and of a hot flame, respectively. Meanwhile, MIE_{prop} (red dotted line) is defined for a self-sustained hot flame, this corresponds to flame type III and IV.

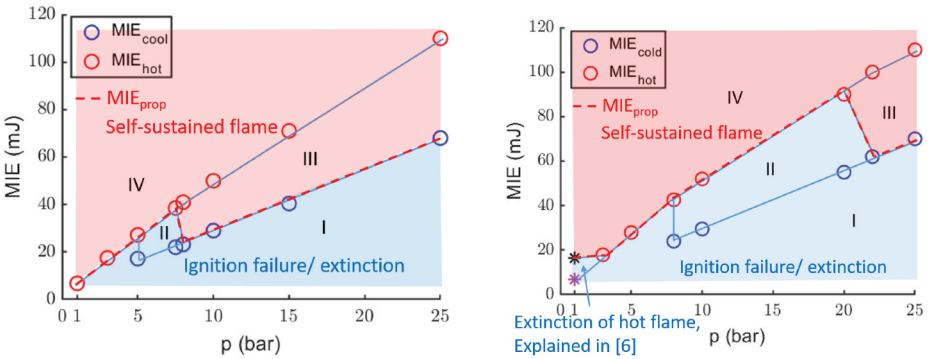

Figure 3. The dependence of MIE on pressure for (a) n-heptane/air and (b) iso-octane/air mixtures, $\phi = 0.8$, $T_0 = 373$K. Red: successful ignition; blue: extinction.

Similar to the simulation results of MIE for hydrogen/oxygen mixtures (Maas U and Warnatz J 1988), the MIE for n-heptane and iso-octane hot flames increases with pressure. However, in experiments (see, e.g., Shy et al. (2017)), a contrary tendency (MIE decreases with increasing pressure) was observed. The reason is that, numerical simulations are performed for constant r_s, resulting in a constant V_s. Consequently, the MIE increases as ρ increases with increasing pressure. On the other hand, in experiments, the gap between the electrodes is adjusted at each pressure to reach the MIE. At elevated pressures, ignition is achieved with a much smaller gap compared to 1 bar, resulting in a smaller ignition volume. The mass of the mixture in the ignition volume shows a decreasing tendency with increasing pressure, and so does the MIE. In simulations, r_s affects the MIE. As shown in Figure 4, at $p = 5$ bar, MIE $= 0.85$ mJ is reached at $r_s = 0.3$ mm. If the ignition radius in simulations is adjusted at each pressure to reach the MIE, the MIE shows a decreasing tendency with increasing pressure, as shown in Figure 5, which is in agreement with the experimental results.

MIE_{cool} is smaller than MIE_{hot} because the temperature required for initiating cool flame reactions is smaller than that for a hot flame. This was also observed for DME/air flames by Ju et al. (Ju 2017). Figure 3 shows that at the same pressure, MIE_{hot} and MIE_{cool} are comparable for iso-octane/air mixtures and n-heptane/air mixtures. For MIE_{hot}, this is consistent with the observation in (Moorhouse et al. 1974), that the MIE of hydrocarbons are similar. For MIE_{cool}, although the LTC of iso-octane is weaker than LTC of n-heptane, the LTC time scale for iso-octane is still faster than the time scale of heat dissipation, so the MIE_{cool} for iso-octane and n-heptane are comparable. The weaker LTC of iso-octane compared to n-heptane might then lead to cool flame extinction due to heat losses, instead of a two-stage ignition.

At 1 bar, the hot flame of iso-octane may quench due to strong diffusion effects, as detailed in our previous study (Wu et al. 2023). At elevated pressures, however, when the ignition radius is kept the same as at 1 bar, the hot flame remains self-sustained, and no hot-flame extinction is observed. This can be understood by noting that at higher pressures,

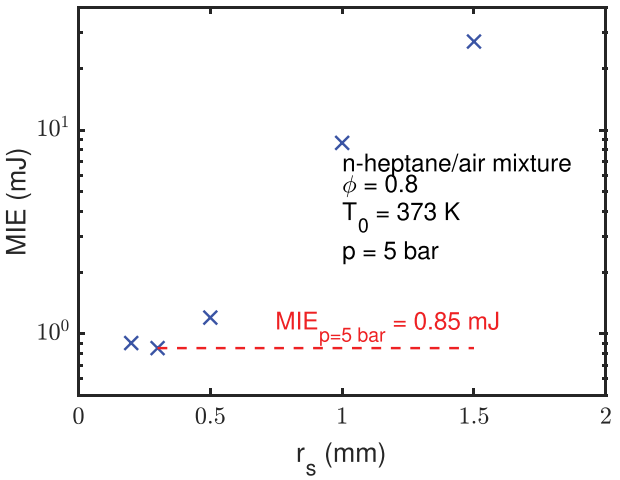

Figure 4. Dependence of MIE on ignition radius for lean n-heptane/air mixtures with $\phi = 0.8$ at $T_0 = 373$ K.

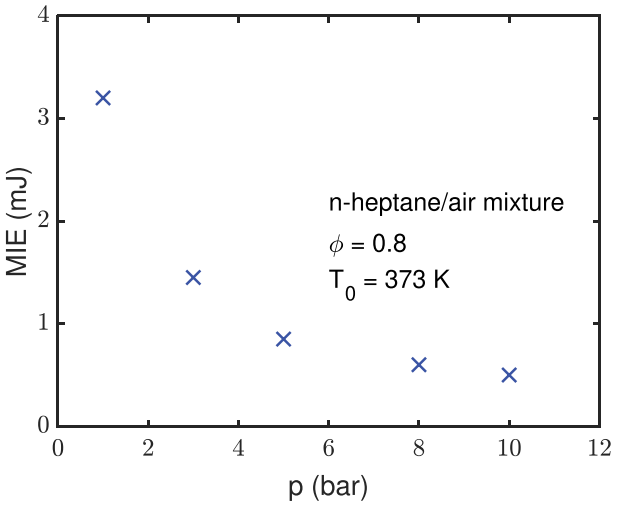

Figure 5. Dependence of MIE on pressure with varying ignition radii for lean n-heptane/air mixtures with $\phi = 0.8$ at $T_0 = 373$ K.

diffusion is slower and chemical reaction is faster than at lower pressure. Flames propagate at fast speed directly after ignition, and are self-sustaining.

As mentioned in Sec. 2, we use the mass-based Lagrangian coordinate Ψ to distinguish flame propagation from pure thermal expansion. The cubic-root of $\Psi_{(r_f)}$ is used here as a space-like coordinate. Figure 6 shows the temporal evolution of $\Psi_{(r_f)}$ for iso-octane/air mixtures at 1 bar and at 3 bar. At 1 bar, after ignition, the flame radius is small, and the curvature is large. Because of the strong diffusion, the flame first propagates slowly and might quench after a while. After reaching a critical flame radius, it propagates with a fast speed and is self-sustained from then on. During the slow flame propagation, the flame quenches if $E_{ig} < MIE_{prop}$, which is the MIE of flame propagation (Wu et al. 2023). In the

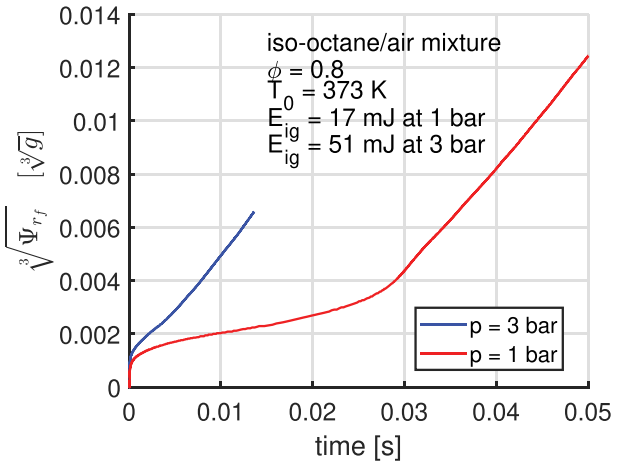

Figure 6. The flame front movement because of chemical reactions for an iso-octane/air flame at 1 bar and at 3 bar.

work of Meyer et al. (1973), they found out that the excitation time decreases by a factor of 100 when pressure is increased from 1 bar to 10 bar. This is another indication for the increase of heat release rate with pressure increase.

Figure 3 shows that there exists a distinct pressure limit p_{lim}, which is defined as the minimum pressure at which LTC-driven ignition is observed. Below p_{lim}, the LTC is too weak to allow formation of cool flames. Spark energy deposition either leads to a self-sustained hot flame, or to an ignition failure. For n-heptane, we found $p_{lim} = 5$ bar and for iso-octane, we found $p_{lim} = 8$ bar. For pressures above p_{lim}, LTC becomes stronger, and cool flames can be formed if $E_{ig} > MIE_{cool}$. However, there is no transition from cool flame to hot flame: the temperature decreases because of heat conduction, and the cool flame quenches. The formation of a self-sustained hot flame requires that $MIE_{prop} = MIE_{cool}$. For the investigated conditions, the transition is sharp within the pressure resolution considered (e.g., no cool-flame ignition at 4.9 bar but present at 5.0 bar for n-heptane). The reported p_{lim} values are conditional and are expected to vary with parameters such as ignition radius, equivalence ratio, and chemical mechanism. Near 8 bar for n-heptane and near 22 bar for iso-octane, a sudden decrease of MIE_{prop} is observed. LTC then is strong enough to allow the cool flame to persist until the second-stage ignition sets in, by which a self-sustained hot flame is formed, $MIE_{prop} = MIE_{cool}$.

The determination of flame type after ignition is summarized in Figure 7. For the case $p < p_{lim}$, if the ignition energy is higher than MIE_{hot}, a self-sustained flame is formed, otherwise ignition failure is observed. For the case $p \geq p_{lim}$, more possibilities exist after ignition energy deposition: If $E_{ig} < MIE_{cool}$, an ignition failure is observed. If $MIE_{cool} \leq E_{ig} \leq MIE_{hot}$, a cool flame is formed. The cool flame can only evolve into a self-sustained hot flame, if $E_{ig} \geq MIE_{prop}$, otherwise the cool flame quenches. If $E_{ig} \geq MIE_{hot}$, a hot flame is directly formed, without the formation of a cool flame.

As shown in Figure 3, both p_{lim} and the pressure where the cool flame can always propagate to a hot flame are smaller for n-heptane than for iso-octane. The main reason

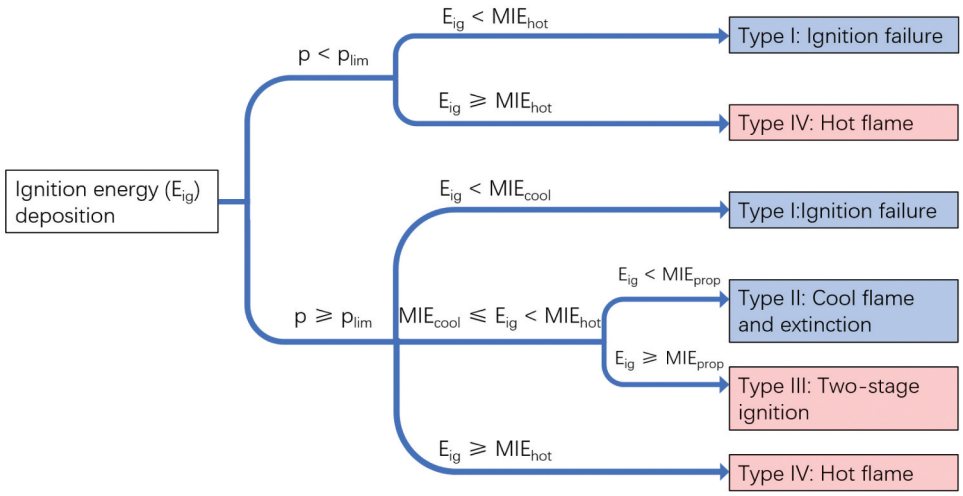

Figure 7. Tree-like classification scheme of different types of evolution after ignition energy deposition. Red: successful ignition; blue: extinction.

is that at the same pressure, the LTC is stronger for n-heptane than for iso-octane. Figure 8 compares the flame structure of n-heptane and iso-octane. It is clearly observed, that with the same ignition energy, although the cool flame temperature of n-heptane is only slightly higher than that of iso-octane, the peaks of the mass fractions of HO_2, H_2O_2, and CH_2O for a n-heptane cool flame are much larger than for an iso-octane cool flame. For the cool-flame regime, the enhanced buildup of HO_2 and H_2O_2 promotes HO $_2$-mediated radical amplification, while the subsequent decomposition of H_2O_2 provides a dominant source of OH radicals for second-stage ignition (Ju 2021). Meanwhile, the higher concentration of CH_2O in n-heptane flame reflects stronger low-temperature oxidation and contributes to sustaining the cool flame. Hence with exactly the same ignition energy, for n-heptane a cool flame survives and triggers a self-sustained hot flame, while the iso-octane cool flame quenches.

Dependence of MIE on RON

Figure 9 shows the dependence of MIE_{prop} on RON at 1 bar (from our previous study (Wu et al. 2023)) and at 10 bar. At 1 bar, MIE_{prop} is nearly independent on RON for small RONs. Near RON = 50, it starts to increase with RON. To check what role LTC plays in this phenomenon, simulations were repeated with a mechanism in which the reactions involving peroxidic radicals involved in LTC were removed. This didn't affect the bend of the MIE_{prop} curve, and implies that at 1 bar, LTC for all PRFs is negligibly weak. The bend is due to the different reaction pathways of n-heptane and iso-octane, as explained in detail in (Wu et al. 2023).

Differences in the dependence of MIE_{prop} on RON between 10 bar and 1 bar are observed. First of all, instead of the existence of a bend, the MIE_{prop} at low RONs depends weakly on RON. From RON = 30 to RON = 50, MIE_{prop} increases rapidly with RON. After that, MIE_{prop} again depends only weakly on RON. Secondly, with the removal of reactions with peroxidic radicals, MIE_{prop} becomes independent on RON throughout the whole region. This implies that at 10 bar, LTC which is dominated by peroxidic radicals has a major effect on the dependence of MIE on RON.

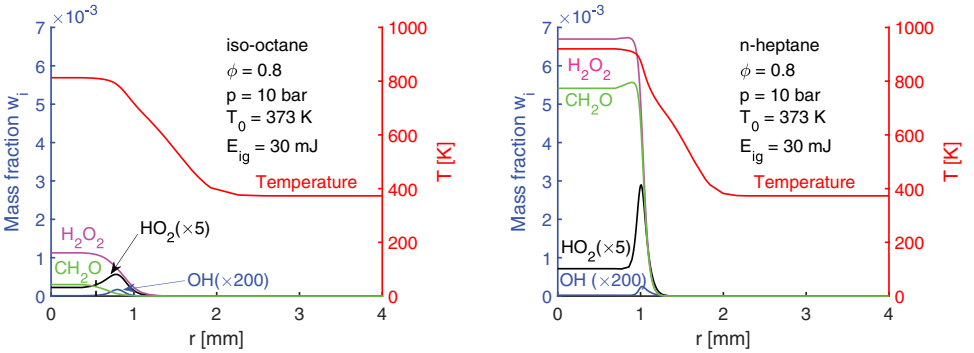

(a) iso-octane cool flame (b) n-heptane cool flame

Figure 8. The flame structure of iso-octane and n-heptane cool flame, including profiles of temperature, and some important species mass fractions.

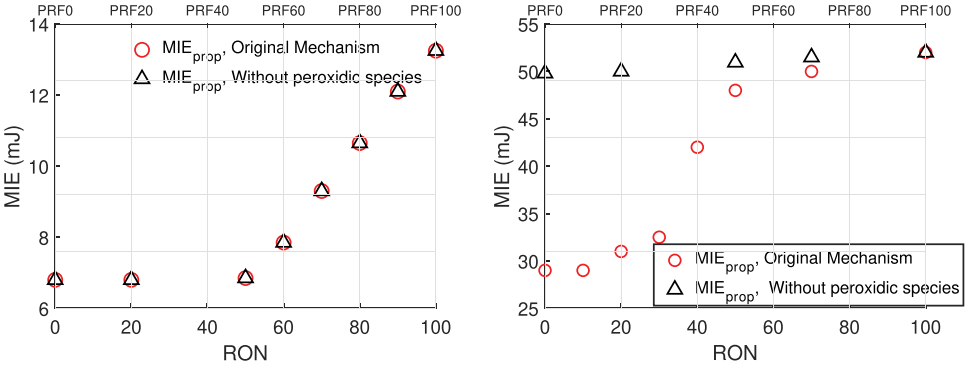

(a) 1 bar (Wu et al., 2023) (b) 10 bar

Figure 9. The dependence of MIE on RON at 1 bar and at 10 bar, with or without peroxidic radicals, $\phi = 0.8$, $T_0 = 373$ K.

The dependence of $\mathrm{MIE_{prop}}$ on RON at different pressures is then investigated. We focus here on $\mathrm{MIE_{prop}}$, because of its technical significance as the minimum energy for a self-sustained flame. To better compare the MIE at different pressures, the specific MIE e_{min} is used here:

$$e_{min} = \frac{\mathrm{MIE_{prop}}}{\rho \cdot V_s} \tag{5}$$

where ρ is the density, and V_s is the volume of the ignition kernel. Results are shown in Figure 10.

The dependence of the e_{min} on RON varies significantly with pressure:

• The dependence of e_{min} on RON at 1 bar originates from extinction caused by strong diffusive losses and different reaction pathways of iso-octane and n-heptane during hot

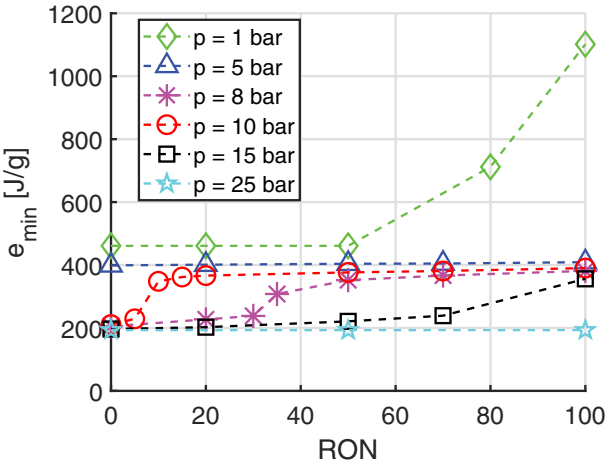

Figure 10. The dependence of $\mathrm{MIE_{prop}}$ on RON for PRF/air mixtures, $\phi = 0.8$, $T_0 = 373$K.

flame combustion. This dependence has been discussed in detail in our previous work (Wu et al. 2021).

- At 5 bar, diffusive effects are weaker, and e_{min} becomes nearly independent of RON.
- When the pressure exceeds 8 bar, MIE is again dependent on RON. This behavior can be explained by the strength of low-temperature chemistry (LTC): for *n*-heptane and PRFs with low RON, LTC is strong enough to promote hot-flame formation, resulting in $MIE_{prop} = MIE_{cool}$. In contrast, for iso-octane and PRFs with high RON, LTC is weak, and the cool flame quenches before transition to a hot flame, giving $MIE_{prop} = MIE_{hot}$. As pressure increases, the LTC of all PRFs becomes stronger, and the critical RON at which e_{min} begins to rise shifts toward RON $\approx$ 100.
- At pressures above 20 bar, even iso-octane exhibits sufficiently strong LTC to allow its cool flame to propagate and evolve into a self-sustained hot flame. Consequently, the dependence of MIE on RON disappears (see, e.g., MIE_{prop} at $p = 25$bar in Figure 10). This insensitivity is expected to be generally valid, as at sufficiently high pressure the cool flame for both iso-octane and n-heptane can always transition to a hot flame. However, the specific pressure at which this behavior occurs may vary depending on the fuel and equivalence ratio.

Conclusions

This study numerically investigated induced ignition and early flame propagation in PRF/air mixtures at pressures from 3 to 25 bar, resolving detailed chemistry and transport processes in space and time. The simulations revealed four distinct ignition regimes: ignition failure, cool flame initiation followed by extinction, two-stage ignition, and direct hot flame initiation.

The results demonstrate that low-temperature chemistry (LTC) plays a decisive role in determining the ignition behavior of PRFs at elevated pressure. LTC enables ignition through a cool flame at temperatures around 700–800 K, considerably lower than those required for hot-flame initiation. The strength of LTC governs whether a cool flame can transition to a self-sustained hot flame or extinguishes after initiation. With increasing pressure, diffusive losses are reduced and LTC becomes stronger, allowing even iso-octane to sustain a hot flame at sufficiently high pressures.

The dependence of the minimum ignition energy (MIE) on RON is thus directly linked to the pressure dependence of LTC activity. At low pressures, strong diffusion causes hot-flame extinction, while at higher pressures, the transition from MIE_{cool} to MIE_{hot} shifts toward larger RON as LTC strengthens across all PRFs. When pressure exceeds about 20 bar, the influence of RON on MIE_{prop} nearly vanishes because even fuels with weak LTC can support self-sustained hot flames.

Overall, this work provides understanding of how low-temperature chemistry, diffusion, and fuel reactivity interact to control ignition and early flame development under elevated pressures. These insights are relevant for optimizing ignition systems in advanced combustion engines and for assessing ignition hazards in high-pressure environments.

Acknowledgements

The authors gratefully acknowledge the financial contribution from the Deutsche Forschungsgemeinschaft (DFG) under the project MA1205/26-1, project number 387641749.

Disclosure statement

No potential conflict of interest was reported by the author(s).

Funding

The work was supported by the Deutsche Forschungsgemeinschaft.

References

Andrae JC. 2008. Development of a detailed kinetic model for gasoline surrogate fuels. Fuel. 870 (10–11):0 2013–2022. https://doi.org/10.1016/j.fuel.2007.09.010

Andrae JC, Brinck T, Kalghatgi GT. 2008. HCCI experiments with toluene reference fuels modeled by a semidetailed chemical kinetic model. Combust Flame. 1550(4):0 696–712.

Andrae JC, Head R. 2009. HCCI experiments with gasoline surrogate fuels modeled by a semidetailed chemical kinetic model. Combust Flame. 1560(4):0 842–851.

Bajwa AU, White SP, Leach FCP. 2025. Low temperature heat release and ø-sensitivity characteristics of iso-octane/air mixtures. Combust Sci Technol. 1970(2):0 440–462.

Bird RB, Stewart WE, Lightfoot EN. 2002. Transport phenomena. 2nd ed. John Wiley & Sons.

Curran H, Gaffuri P, Pitz W, Westbrook C. 1998a. A comprehensive modeling study of n-heptane oxidation. Combust Flame. 1140(1):0 149–177.

Curran H, Gaffuri P, Pitz W, Westbrook C. 2002. A comprehensive modeling study of iso-octane oxidation. Combust Flame. 1290(3):253–280.

Curran H, Pitz W, Westbrook C, Callahan G, Dryer F. 1998b. Oxidation of automotive primary reference fuels at elevated pressures. Proc Combust Inst. 270(1):379–387.

Dagaut P, Togbé C. 2009. Experimental and modeling study of the kinetics of oxidation of butanol-n-heptane mixtures in a jet-stirred reactor. Energy Fuels. 230(7):3527–3535.

Davis S, Law C. 1998. Laminar flame speeds and oxidation kinetics of iso-octane-air and n-heptane-air flames. Proc Combust Inst. 270(1):521–527.

Dunn-Rankin D. 2011. Lean combustion: technology and control. Academic Press.

Edgar G. 1927. Measurement of knock characteristics of gasoline in terms of a standard fuel. Ind Eng Chem. 190(1):145–146.

Griffiths J, MacNamara J, Sheppard C, Turton D, Whitaker B. 2002. The relationship of knock during controlled autoignition to temperature inhomogeneities and fuel reactivity. Fuel. 810 (17):2219–2225. https://doi.org/10.1016/S0016-2361(02)00134-5

Griffiths J, Scott S. 1987. Thermokinetic interactions: Fundamentals of spontaneous ignition and cool flames. Prog Energy Combust Sci. 130(3):161–197.

Hirschfelder JO, Curtiss CF, Bird RB. 1964. Molecular theory of gases and liquids. John Wiley & Sons.

Ju Y. 2017. On the propagation limits and speeds of premixed cool flames at elevated pressures. Combust Flame. 178:0 61–69. https://doi.org/10.1016/j.combustflame.2017.01.006

Ju Y. 2021. Understanding cool flames and warm flames. Proc Combust Inst. 380(1):83–119.

Ju Y, Sun W, Burke MP, Gou X, Chen Z. 2011. Multi-timescale modeling of ignition and flame regimes of n-heptane-air mixtures near spark assisted homogeneous charge compression ignition conditions. Proc Combust Inst. 330(1):1245–1251.

Kelley A, Liu W, Xin Y, Smallbone A, Law C. 2011. Laminar flame speeds, non-premixed stagnation ignition, and reduced mechanisms in the oxidation of iso-octane. Proc Combust Inst. 330 (1):501–508.

Kumar K, Freeh JE, Sung CJ, Huang Y. 2007. Laminar flame speeds of preheated iso-octane/O2/N2 and n-heptane/O2/N2 mixtures. J Propul Power. 230(2):428–436.
Lewis B, Von Elbe G. 2012. Combustion, flames and explosions of gases. Elsevier.
Liang W, Law CK. 2017. Extended flammability limits of n-heptane/air mixtures with cool flames. Combust Flame. 185:75–81. https://doi.org/10.1016/j.combustflame.2017.06.015
Maas U, Raffel B, Wolfrum J, Warnatz J. 1988. Observation and simulation of laser induced ignition processes in O2-O3 and H2-O2 mixtures. Proc Combust Inst. 210(1):1869–1876.
Maas U, Warnatz J. 1988. Ignition processes in hydrogen-oxygen mixtures. Combust Flame. 740 (1):53–69.
Meyer JW, Cohen LM, Oppenheim AK. 1973. Study of exothermic processes in shock ignited gases by the use of laser shear interferometry. Combust Sci Technol. 80(4):185–197.
Moorhouse J, Williams A, Maddison T. 1974. An investigation of the minimum ignition energies of some C1 to C7 hydrocarbons. Combust Flame. 230(2):203–213.
Müller U, Peters N, Liñán A. 1992. Global kinetics for n-heptane ignition at high pressures. Proc Combust Inst. 240(1):777–784.
Pan J, Wei H, Shu G, Chen Z, Zhao P. 2016. The role of low temperature chemistry in combustion mode development under elevated pressures. Combust Flame. 174:179–193. https://doi.org/10.1016/j.combustflame.2016.09.012
Paul P, Warnatz J. 1998. A re-evaluation of the means used to calculate transport properties of reacting flows. Symp (Int) Combust. 270(1):495–504.https://doi.org/10.1016/S0082-0784(98)80439-6
Peters N, Paczko G, Seiser R, Seshadri K. 2002. Temperature cross-over and non-thermal runaway at two-stage ignition of n-heptane. Combust Flame. 1280(1):38–59.
Shy S, Shiu Y, Jiang L, Liu C, Minaev S. 2017. Measurement and scaling of minimum ignition energy transition for spark ignition in intense isotropic turbulence from 1 to 5 atm. Proc Combust Inst. 360(2):1785–1791.
Sim HS et al. 2025. Experimental and numerical study of ignition and combustion processes of primary reference fuels for advanced compression-ignition applications. Energy Convers Manag. 346:120361. https://doi.org/10.1016/j.enconman.2025.120361
Sim HS, Maes N, Pickett LM, Skeen SA, Manin J. 2023. High-speed formaldehyde planar laser-induced fluorescence and schlieren to assess influences of injection pressure and oxygen concentration on spray a flames. Combust Flame. 253:112806. https://doi.org/10.1016/j.combustflame.2023.112806
Sim HS, Maes N, Weiss L, Pickett LM, Skeen SA. 2021. Detailed measurements of transient two-stage ignition and combustion processes in high-pressure spray flames using simultaneous high-speed formaldehyde PLIF and schlieren imaging. Proc Combust Inst. 380(4):5713–5721.
Sim HS, Weiss L, Maes N, Pickett LM. 2024. High spatiotemporal resolution optical measurements of two-stage ignition and combustion in engine combustion network spray D flames. Case Stud Therm Eng. 62:105192. https://doi.org/10.1016/j.csite.2024.105192
Stagni A et al. 2018. The influence of low-temperature chemistry on partially-premixed counter-flow n-heptane/air flames. Combust Flame. 188:440–452. https://doi.org/10.1016/j.combustflame.2017.10.002
Sun W, Won SH, Gou X, Ju Y. 2015. Multi-scale modeling of dynamics and ignition to flame transitions of high pressure stratified n-heptane/toluene mixtures. Proc Combust Inst. 350 (1):1049–1056.
Tanoue K, Jimoto T, Kimura T, Yamamoto M, Hashimoto J. 2017. Effect of initial temperature and fuel properties on knock characteristics in a rapid compression and expansion machine. Proc Combust Inst. 360(3):3523–3531.
Uchman W, Werle S. 2018. The ignition phenomenon of gases—part I: The experimental analysis—a review. J Power Technol. 980(2)
Warnatz J, Maas U, Dibble R. 2006a. Combustion: physical and chemical fundamentals, modeling and simulation, experiments, pollutant formation. Berlin, Heidelberg: Springer.
Warnatz J, Maas U, Dibble RW. 2006b. Combustion: physical and chemical fundamentals, modeling and simulation, experiments, pollutant formation. 4th ed. Springer.

Wu C, Chen Y-R, Schießl R, Shy SS, Maas U. 2023. Numerical and experimental studies on minimum ignition energies in primary reference fuel/air mixtures. Proc Combust Inst. 390(2):1987–1996.
Wu C, Schießl R, Maas U. 2021. Numerical studies on minimum ignition energies in methane/air and iso-octane/air mixtures. J Loss Prevent Proc. 72:104557. https://doi.org/10.1016/j.jlp.2021.104557
Yin P, Liu W, Yang Y, Gao H, Zhang C. 2022. An experimental and modeling study on the combustion of gasoline-ethanol surrogates for HCCI engines. Secur Commun Netw. 2022:1–10. https://doi.org/10.1155/2022/5362928
Zhong S et al. 2020. Structure and propagation of n-heptane/air premixed flame in low temperature ignition regime. Appl Energy. 275:115320. https://doi.org/10.1016/j.apenergy.2020.115320